

Effect of Toughness Distribution in the Thickness Direction on Brittle Crack Propagation/Arrest Behavior of Heavy-gauge Steel Plate[†]

HANDA Tsunehisa^{*1} NISHIMURA Kimihiro^{*2} TSUYAMA Seishi^{*3}

Abstract:

Brittle crack arrestability of heavy steel plates with different toughness distribution in the plate thickness direction was investigated to clarify the optimum distribution of properties in the thickness direction, which is necessary in the development of heavy steel plates with excellent brittle crack arrest performance. Ultra-wide duplex ESSO tests were performed, and the effect of the toughness distribution in the thickness direction on the arrestability of long brittle cracks was studied. Even in plates having the same brittle crack arrest toughness value, plates in which the toughness at the middle thickness position ($1/2t$) is higher than that at the $1/4t$ and surface layer positions displayed higher brittle crack arrestability under no temperature gradient condition which simulates actually applications, than plates in which the $1/2t$ toughness is lower than that at the $1/4t$ and surface positions. Furthermore, it is shown that this superiority is maintained even in the case of long brittle cracks.

1. Introduction

In recent years, large-scale container ships exceeding 10 000 TEU have been constructed in order to improve transportation efficiency^{1,2)} (TEU: Twenty-foot equivalent unit; unit expressing cargo capacity as a number of 20-foot-long containers). Due to the hull structure of container ships, high strength, heavy-gauge plates are

increasingly used in strength decks and hatch side coamings, which are superstructure structural members. Recently, yield point of 390 N/mm² class steel and 460 N/mm² class steel with plate thicknesses exceeding 70 mm have been applied³⁻⁵⁾.

Because ships are welded structures, in the unlikely event that a brittle crack initiates from a weld, the basic concept is to arrest its propagation and thereby prevent failure of the ship as a whole. Much research, including large-scale demonstration experiments, has been devoted to the brittle crack arrestability of heavy-gauge plates used in ship structures⁶⁻¹¹⁾, and guidelines have been presented indicating that the brittle crack arrest toughness, K_{Ic} , of steel plates at the ship design temperature of -10°C should be at least 6 000 N/mm^{3/2} or more in order to arrest a long brittle crack that has propagated rectilinearly along a weld in the base metal of a heavy-gauge steel plate with a thickness exceeding 50 mm¹²⁾. International regulations have also been issued¹³⁾, and steel material manufacturers have been asked to develop heavy-gauge steel plates with excellent brittle crack arrest performance.

The properties of heavy-gauge materials are not necessarily uniform in the plate thickness direction. Toughness, which is considered to govern brittle crack arrestability, also varies in the thickness direction. Although control of the toughness distribution in the thickness direction is conceivable as one means of improving arrestability, there have been few examples of research

[†] Originally published in JFE GIHO No. 33 (Feb. 2014), p. 43–48



^{*1} Dr. Eng.,
Senior Researcher Manager,
Joining & Strength Res. Dept.,
Steel Res. Lab.,
JFE Steel



^{*2} Staff General Manager,
Plate Business Planning Dept.,
JFE Steel



^{*3} Dr. Eng.,
Senior Vice President,
General Superintendent, Steel Res. Lab.,
JFE Steel

on the effect of this kind of property distribution on the brittle crack arrestability required in actual structures. Therefore, in the present research, the brittle crack arrestability of heavy materials with different toughness distributions in the thickness direction was evaluated in order to clarify the optimum distribution of properties in the plate thickness direction, which is necessary in the development of heavy steel plates with excellent crack arrest performance, and the effect of the toughness distribution on long brittle crack arrestability was verified by performing ultra-wide duplex ESSO tests.

2. Effect of Thickness Direction Toughness Distribution on Arrestability of Heavy-gauge Steel Plates

2.1 Tested Steels

As the tested steels, yield point of 355 N/mm² class heavy steel plates with a thickness of 60 mm were used. The mechanical properties of the steels are shown in **Table 1**. Steel A was a material that was manufactured so that toughness in the Charpy impact test decreased in the order of surface layer, 1/4 t , and 1/2 t . Conversely, Steels B and C were manufactured so that the toughness increased in the same order, i.e., from the surface layer to the 1/4 t and 1/2 t positions.

2.2 Brittle Crack Arrestability of Tested Steels

The temperature gradient ESSO test (Kca test) was performed in order to determine the brittle crack arrestability, Kca, of the tested steels. The test method conformed to the Kca test method¹²⁾.

Figure 1 shows the results of the temperature gradient ESSO test. The Kca values at the ship design temperature of -10°C were 4 400 N/mm^{3/2} for Steel A, 7 200 N/mm^{3/2} for Steel B, and 6 500 N/mm^{3/2} for Steel C. As shown in **Photo 1**, the distinctive feature here is the fact that the fracture surface morphology of Steel A displays the general thumb-nail shape, in which the crack propagates at the middle thickness position in comparison to the surface layer, whereas Steels B and C display a split-nail-shaped pattern, in which cracks propagate at the 1/4 t and 3/4 t positions before the middle

Table 1 Mechanical properties of steel plates tested

Steel	Thickness (mm)	YS (N/mm ²)	TS (N/mm ²)	vTrs (°C)		
				1/2 t	1/4 t	Surface
A	60	375	525	-36	-70	-85
B		389	491	-108	-84	-73
C		393	491	-111	-106	-87

YS: Yield strength TS: Ultimate tensile strength
vTrs: Charpy transition temperature

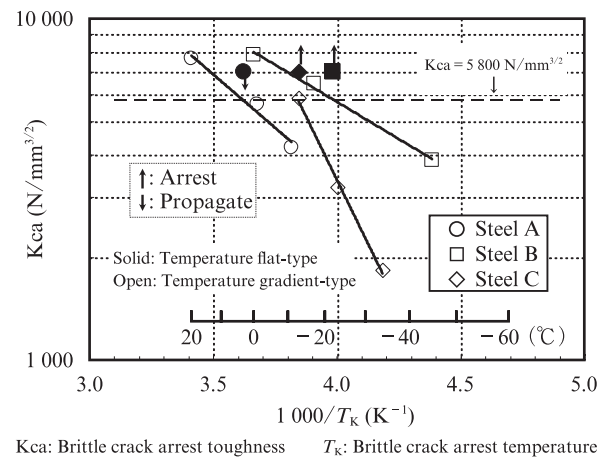


Fig. 1 Comparison of flat temperature-type ESSO test results and temperature gradient ESSO test results

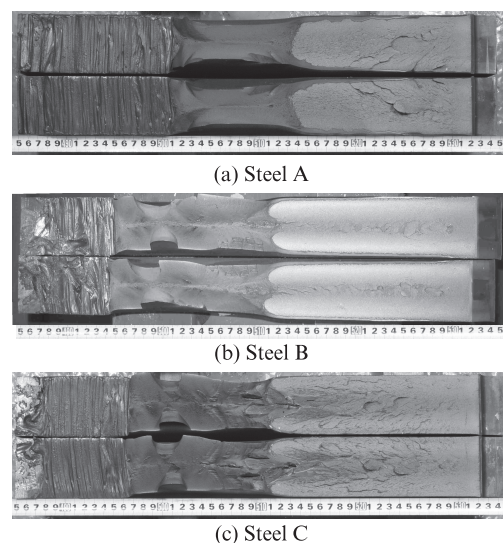


Photo 1 Example of fracture appearance of ESSO test specimen

thickness position.

2.3 Arrestability of Tested Steels under No-Temperature-Gradient Condition

2.3.1 Flat-temperature type ESSO test

Brittle crack arrestability, Kca, is normally measured under the condition of a temperature gradient of approximately 0.25–0.35°C/mm¹²⁾. In reality, however, steel plates are frequently used under a constant temperature condition. Therefore, a flat-temperature type ESSO test¹⁴⁾ was performed in order to evaluate brittle crack arrestability under a condition of no temperature gradient, which is closer to reality. **Figure 2** shows the geometry of the test specimen and the test method. In order to initiate a brittle crack, as in the temperature gradient ESSO test, a temperature gradient of 0.3°C/mm was given to the upper half of the specimen (half where crack initiation occurs) to reduce the temperature of the

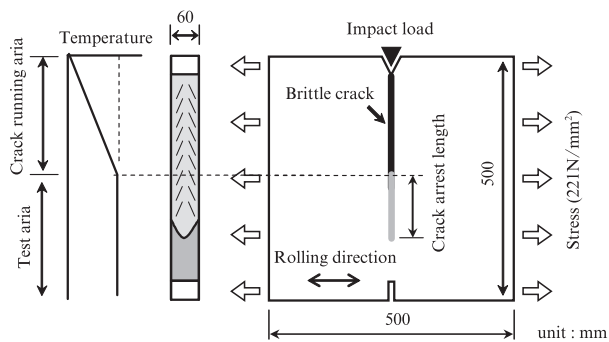


Fig. 2 Flat temperature-type ESSO test method

crack initiation site (notch). The temperature was constant without a gradient in the lower half of the specimen, which is the test area.

In general, it is thought that brittle cracks will be arrested under actual conditions if the K_{Ic} of a steel plate is $6\,000\text{ N/mm}^{3/2}$ or higher⁶⁻¹². The purpose of this research was to investigate the effect of the toughness distribution in the plate thickness direction on brittle crack propagation and arrest behavior. Therefore, when performing the flat-temperature type ESSO test, stress loading of 221 N/mm^2 was applied so that the applied stress intensity factor, K , of a brittle crack penetrating into the test area was $7\,000\text{ N/mm}^{3/2}$, which is more than $6\,000\text{ N/mm}^{3/2}$, and the temperature of the test area was set to a temperature at which the K_{Ic} of the test area would be $5\,800\text{ N/mm}^{3/2}$, which is slightly lower than $6\,000\text{ N/mm}^{3/2}$, so that the brittle crack would propagate to some degree in the test area.

2.3.2 Results of flat-temperature type ESSO test

The results of the flat-temperature type ESSO test are shown in **Table 2** and Fig. 1. Under the temperature condition in which K_{Ic} showed a value of $5\,800\text{ N/mm}^{3/2}$, in Steel A, the brittle crack penetrated completely through the test specimen without arrest in the test area. In contrast to this, in Steel B and Steel C, the brittle cracks propagated in the test area to distances of 70 mm and 30 mm, respectively, after which they were arrested within the test area. Because the fracture driving force under the conditions of the flat-temperature type ESSO test is set higher than in the temperature gradient ESSO test, brittle cracks should propagate in the flat-temperature type ESSO test. However, in these results, propagation only occurred in Steel A, and the brittle cracks were arrested in Steel B and Steel C.

Photo 2 shows a comparison of the fracture surfaces of the flat-temperature type ESSO test specimens and the fracture surfaces of the temperature gradient type. The fracture surfaces of the flat-temperature type ESSO test specimens of Steel B and Steel C display the same split-nail-shaped morphology as the temperature gradi-

Table 2 Results of flat temperature-type ESSO test

Steel	Thickness (mm)	Test condition				Test result
		Stress (N/mm ²)	K^* (N/mm ^{3/2})	Temperature (°C)	K_{Ic}^{*2} (N/mm ^{3/2})	
A	60	221	7 000	3	5 800	Propagate
B				-22		Arrest
C				-13		Arrest

*1 Applied stress intensity factor (Fracture driving force)

*2 Brittle crack arrest toughness K_{Ic} of test area

Steel	Temperature gradient ESSO test	Temperature flat-type ESSO test
A		
B		
C		

Photo 2 Comparison of crack arresting appearance of temperature gradient ESSO specimens and that of flat temperature-type ESSO specimen

ent test specimens, but the degree of crack growth around the $1/4t$ and $3/4t$ positions, relative to that at the middle thickness position, was remarkable in comparison with the temperature gradient type specimens.

As described above, by examining brittle crack propagation/arrest behavior with various toughness distributions in the plate thickness direction, this investigation clarified the fact that the arrestability characteristics of the total plate thickness change, even under the same K_{Ic} condition. In particular, a steel plate in which $1/2t$ toughness is higher than surface toughness and $1/4t$ toughness will display higher brittle crack arrestability under a no-temperature-gradient condition, which simulates actual use, in comparison with a plate in which $1/2t$ toughness is lower than surface toughness and $1/4t$ toughness.

3. Verification of Effect of Thickness Direction Toughness Distribution on Long Brittle Crack Arrestability

In an actual structure, in the unlikely event that a brittle crack occurs, it may conceivably propagate over a long distance and become a long brittle crack⁶. In this

chapter, a large-scale test (ultra-wide duplex ESSO test¹²⁾) was performed, and the effect of the thickness direction toughness distribution on the arrestability of long brittle cracks was verified.

3.1 Ultra-wide Duplex ESSO Test Method

The tested steels are Steel A and Steel C. In preparing the test specimens, an electro-gas welding joint (Plate thickness: 60 mm) was used as the crack running plate, in which a brittle crack was made to initiate and propagate, in order to avoid crack branching during propagation, and butt welding of the crack running plate and the test plate was performed by full penetration CO₂ arc welding. The ultra-wide duplex ESSO test specimen shown in Fig. 3 was then machined from the prepared welded joint. A window-frame type machined notch¹²⁾ was used as the initial notch of the test specimen in order to avoid deviation of the crack from the weld due to weld residual stress.

For the tab plates set between the testing machine and the test specimen, plates having the same thickness as the test specimen were selected, and the distance between the loading points was set at 10 m in order to minimize load drop during the test and reflection of stress waves between the tab plates and the test specimen. The fact that these test conditions gave load conditions that were basically equivalent to actual conditions, in which stress reflection does not occur, was confirmed by a dynamic finite element method (FEM) analysis¹⁵⁾. A testing machine with a capacity of 80 MN was used in this test. As in the flat-temperature type ESSO test, the test specimens were cooled to a temperature at which the Kca of the test plates showed a value of 5 800 N/mm^{3/2}, and were then held at that temperature from 60 min or longer, after which a load equivalent to nominal stress of 257 N/mm² was applied, this being the maximum allowable stress of a steel plate whose yield point is 390 N/mm² class. A brittle crack was initiated and made

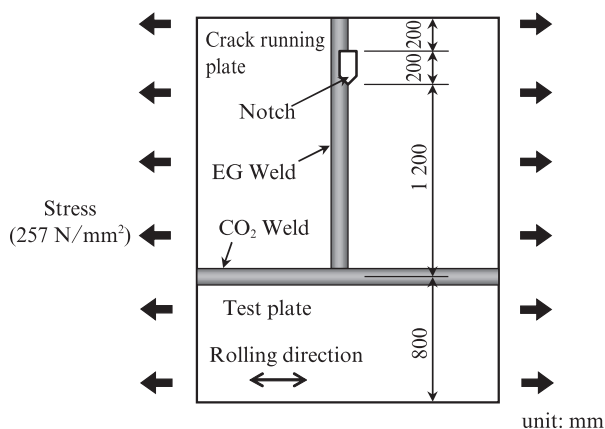
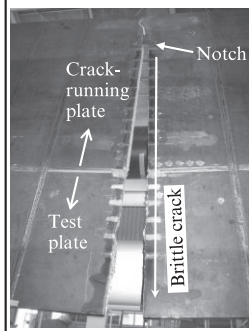
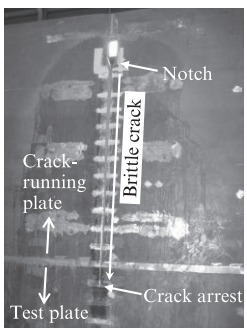
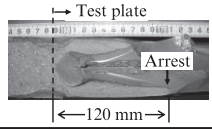


Fig. 3 Dimension of ultra-wide duplex ESSO test specimen

Steel	A	C
Test temperature (°C)	3	-13
Applied stress (N/mm ²)	257	
Kca at test temperature (N/mm ^{3/2})	5 800	
Crack path of the ultra-wide duplex ESSO test		
Fracture surface around the crack arrest position		
Result	Propagate	Arrest

Kca: Brittle crack arrest toughness

Photo 3 Results of ultra-wide duplex ESSO test

to propagate by applying impact to the machined notch part.

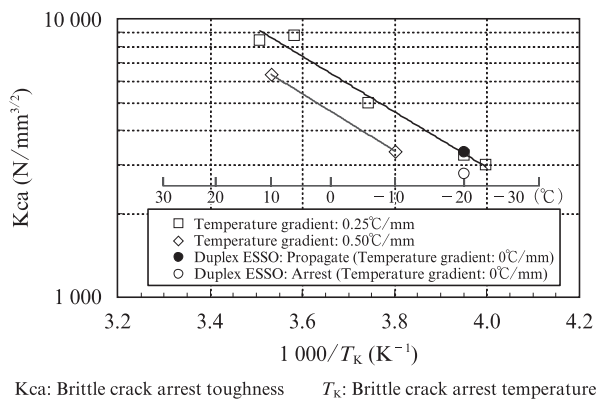
3.2 Results of Ultra-wide Duplex ESSO Test

Photo 3 shows the results of the ultra-wide duplex ESSO test. Under the temperature condition in which Kca was 5 800 N/mm^{3/2}, a long brittle crack penetrated through the full thickness of the test plate of Steel A without arrest. In contrast to this, with Steel C, the brittle crack propagated approximately 120 mm and was then arrested within the test plate. It was confirmed that the fracture surface of Steel C also displayed the same remarkable split-nail-shaped morphology as in the flat-temperature type ESSO test.

4. Discussion of Effect of

Thickness Direction Toughness Distribution on Brittle Crack Arrestability

From the results in Chapter 2, arrestability in the full plate thickness varies, even under the same Kca condition, depending on changes in the toughness distribution in the thickness direction. Specifically, given the no-temperature-gradient condition simulating the condition under which steel materials are actually used, these results clarified that fact a steel plate in which the performance of the 1/2t position is higher than that of the 1/4t position displays higher brittle crack arrestability than a plate in which the performance of the 1/2t posi-

Fig. 4 Effect of temperature gradient on Kca⁷⁾

tion is lower than that of the $1/4t$ position. Furthermore, the results of the ultra-wide duplex ESSO test in Chapter 3 confirmed that this difference is maintained even in the unlikely case that a brittle crack occurs and grows into a long brittle crack in an actual structure. The following discusses the cause of the above-mentioned difference.

First, the results of a comparison of the temperature gradient ESSO test and the flat-temperature type ESSO test will be considered. As mentioned previously, the fracture driving force under the temperature condition of the flat-temperature type ESSO test is set higher than that in the temperature gradient ESSO test. Therefore, a brittle crack should propagate in the flat-temperature type ESSO test. However, propagation occurred only in Steel A, and the brittle cracks were arrested in Steel B and Steel C. As the cause of this difference, it is thought that the temperature gradient in the test area affected the measured values of brittle crack toughness (Kca)⁷⁾. **Figure 4** shows an example⁷⁾ of an investigation of the effect of the temperature gradient in the test area on the measured values of brittle crack toughness (Kca). The test specimen is a yield point of 355 N/mm² class thick plate with a thickness of 50 mm. This is a steel in which the brittle crack arrest area shows the general thumb-nail-shaped fracture surface morphology, like that observed in Steel A used in this research. With this kind of general steel, brittle crack toughness (Kca) increases as the temperature gradient decreases, and at a temperature gradient of 0.25°C/mm, the Kca value can be evaluated as being the same as that under the no-temperature-gradient condition simulating the actual condition.

The fact that the brittle crack toughness (Kca) is affected by the temperature gradient is considered to be due to a change in the fracture surface morphology depending on the temperature gradient, as shown in **Fig. 5**. During propagation, a brittle crack is a through-thickness crack, in which the crack front is substantially linear¹⁶⁾. Therefore, if a toughness distribution exists in the plate thickness direction, it is thought that the brittle

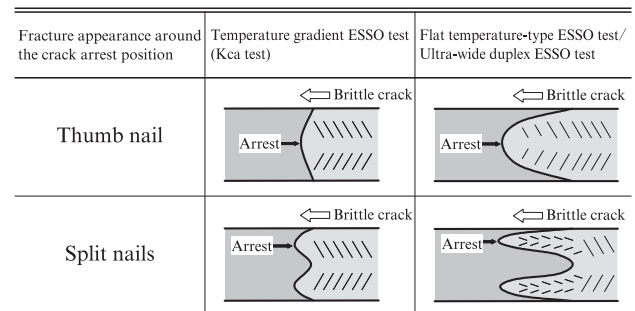


Fig. 5 Schematic illustration about effect of temperature gradient on fracture surface of ESSO test specimen

crack will be arrested first in the part where toughness is relatively high, and arrest will be delayed at positions of relatively lower toughness. In this case, if a temperature gradient exists, the brittle crack will be arrested in the high toughness part, after which the crack in the low toughness part will penetrate into the higher temperature part (i.e., higher toughness part), and as a result, the crack will be arrested in a shorter distance than when no temperature gradient exists. Thus, as shown in Fig. 5, the difference in the crack arrest position will become smaller; consequently, the crack tip shape will become more linear than under a condition of no temperature gradient.

The Kca test method¹²⁾ specifies a temperature gradient range of 0.25–0.35°C/mm in order to avoid under-evaluating Kca due to change in the fracture surface morphology. In the Kca test (ESSO test with temperature gradient of 0.3°C/mm), the Kca value of Steel A used in this research was evaluated as the same as that under the no-temperature-gradient condition (actual condition) because it showed the general thumb-nail-shaped fracture surface. Thus, it can be interpreted that the brittle crack propagated as in the flat-temperature type ESSO test, in which the fracture driving force is set high, as shown in Fig. 1.

In contrast, in Steel B and Steel C, which displayed the split-nail-shaped fracture surface morphology, it can be estimated that the Kca value of the temperature gradient ESSO test is smaller than that under the no-temperature-gradient condition (actual condition). However, since this gives a conservative evaluation, the evaluation of Kca of these steels by the temperature gradient ESSO test presents no problems for practical application. As shown in Photo 2, in steels that display the split-nail-shaped fracture surface morphology, the fracture surface morphology of the crack arrest area differs greatly in the Kca test (ESSO test with temperature gradient of 0.3°C/mm) and the flat-temperature type ESSO test. This difference is shown schematically in Fig. 5 in comparison with the case of the general thumb-nail-shaped fracture surface. Although the brittle crack arrest position is nor-

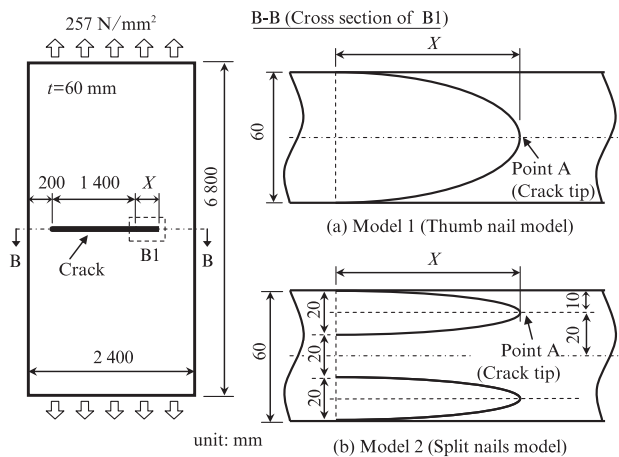


Fig. 6 Finite element method (FEM) models for calculation of stress intensity factor

mally defined by the area where the longest propagation occurred¹²⁾, there is a possibility that the value of the stress intensity factor (fracture driving force) at the crack tip differs greatly depending on the fracture surface morphology. Therefore, the stress intensity factor at the crack tip was evaluated by an FEM analysis. **Figure 6** shows the models of the FEM analysis. The object of the analysis was the ultra-wide duplex ESSO test. Two models were analyzed, namely, Model 1, which simulates the general thumb-nail-shaped fracture surface morphology, where the crack advances at the plate middle thickness position in comparison with the surface layer, and Model 2, which simulates the split-nail-shaped fracture surface morphology, where the crack advances at the $1/4t$ and $3/4t$ positions before the middle thickness position. In order to investigate changes of the fracture driving force (stress intensity factor) at the tip of a long brittle crack which has propagated in the crack running plate after it penetrates the test plate, the crack tip position was changed to 0, 50, 100, or 250 mm from the boundary between running plate and test plate to the test plate side. The model was a perfect elastic body (Young's modulus=206 000 N/mm², Poisson's ratio=0.3), to which tensile stress of 257 N/mm² was applied. The stress intensity factor was obtained by conversion of the integrated value of J obtained from the FEM analysis.

Figure 7 shows the results of an analysis of the decrease in the stress intensity factor depending on the fracture surface morphology. If it is assumed that, after penetrating the test plate, a crack propagates centering on the $1/4t$ position and does not advance in the surface layer and at the middle thickness position (i.e., the crack propagates like the split-nail-shaped crack of Model 2), the stress intensity factor around the $1/4t$ position will decrease as that crack advances. For example, if the difference in the crack length is 100 mm, the stress intensity factor of the split-nail-shaped crack will decrease to

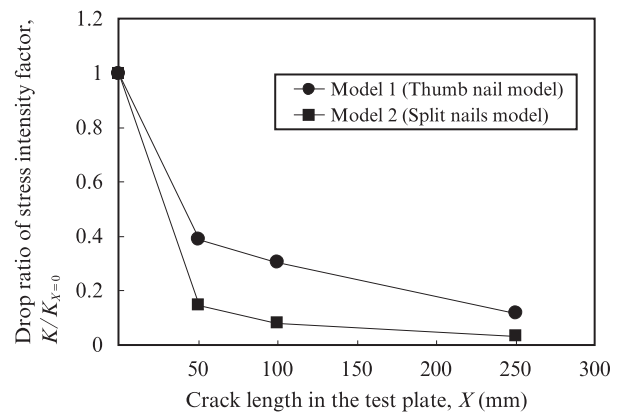


Fig. 7 Relationship between crack length in the test plate X and drop ratio of stress intensity factor obtained by finite element method (FEM) analysis

less than one-half that of the general thumb-nail-shaped crack (Model 1), which means the crack can be arrested more easily. On the other hand, if the crack tip is located at the plate middle thickness position, and the crack does not advance at the normal surface layer, the decrease in the stress intensity factor accompanying crack growth will be small in comparison with the material that shows the split-nail-shaped fracture surface morphology, and crack propagation will occur comparatively easily.

From the above, in steel plates with high toughness in the plate middle thickness in comparison with the surface layer and $1/4t$ positions, like Steel B and Steel C, the brittle crack arrest area will display a split-nail-shaped fracture surface, and the stress intensity factor at the brittle crack tip will also show a larger decrease than that in steels with the general thumb-nail-shaped fracture surface, like Steel A. Thus, particularly under a condition in which virtually no temperature gradient exists, like that in which steel materials are actually used, a toughness distribution characterized by higher toughness in the middle thickness part is considered to be an advantage for brittle crack arrest.

5. Conclusion

In order to clarify the optimum distribution of properties in the plate thickness direction, which is necessary in the development of heavy steel plates with excellent brittle crack arrest performance, the brittle crack arrest characteristics of heavy-gauge materials with different toughness distributions in the thickness direction were evaluated, and the effect of the toughness distribution on brittle crack arrestability was verified by performing ultra-wide duplex ESSO tests. The following knowledge was obtained.

- (1) In steel plates with high toughness in the middle thickness ($1/2t$) position in comparison with the $1/4t$

position, the brittle crack arrest area displayed a split-nail-shaped fracture surface morphology.

- (2) When compared under the same Kca condition, plates that displayed the split-nail-shaped fracture surface morphology, in which the toughness of the $1/2t$ position was higher than that of the $1/4t$ position, showed higher brittle crack arrestability under a no-temperature-gradient condition, which simulates the condition in which steel materials are actually used, than plates in which the toughness of the $1/2t$ was lower than that of the $1/4t$ position.
- (3) Regarding the superiority of plates that display this split-nail-shaped fracture surface morphology, the fact that these plates maintain the split-nail-shaped morphology, even if a brittle crack grows into a long brittle crack in an actual structure, was verified by performing ultra-wide duplex ESSO tests.
- (4) The fact that steel plates in which the brittle crack arrest area displays the split-nail-shaped fracture surface show higher brittle crack arrestability under a no-temperature-gradient condition than plates with the general thumb-nail-shaped fracture surface is attributed to the more remarkable decrease in the stress intensity factor due to crack propagation at the crack tip in plates with the split-nail-shaped fracture surface.

References

- 1) Nagatsuka, S. KANRIN. 2007-03, no. 11, p. 10.
- 2) E.g. <http://www.ship-technology.com/projects/triple-e-class/>
- 3) Mori, S.; Tanaka, S.; Tanaka, Y.; Hirota, K. KANRIN. 2009-05, no. 24, p. 18.
- 4) Nishimura, K.; Handa, T.; Hashimoto, M. JFE Giho. 2007-11, no. 18, p. 18.
- 5) Ichimiya, K.; Sumi, H.; Hirai, T. JFE Technical Report. 2008-06, no. 11, p. 7.
- 6) Yamaguchi, Y.; Yajima, H.; Aihara, S.; Yoshinari, H.; Hirota, K.; Toyoda, M.; Kiyosue, T.; Tanaka, S.; Okabe, T.; Kageyama, K.; Funatsu, Y.; Handa, T.; Kawabata, T.; Tani, T. ISOPE-2010. p. 71.
- 7) Kawabata, T.; Matsumoto, K.; Ando, T.; Yajima, H.; Aihara, S.; Yoshinari, H.; Hirota, K.; Toyoda, M.; Kiyosue, T.; Inoue, T.; Handa, T.; Tani, T. ISOPE-2010. p. 80.
- 8) Handa, T.; Matsumoto, T.; Yajima, H.; Aihara, S.; Yoshinari, H.; Hirota, K.; Toyoda, M.; Kiyosue, T.; Inoue, T.; Kawabata, T.; Tani, T. ISOPE-2010. p. 88.
- 9) Inoue, T.; Yamaguchi, Y.; Yajima, H.; Aihara, S.; Yoshinari, H.; Hirota, K.; Toyoda, M.; Kiyosue, T.; Handa, T.; Kawabata, T.; Tani, T. ISOPE-2010. p. 95.
- 10) Kubo, A.; Yajima, H.; Aihara, S.; Yoshinari, H.; Hirota, K.; Toyoda, M.; Kiyosue, T.; Inoue, T.; Handa, T.; Kawabata, T.; Tani, T.; Yamaguchi, Y. ISOPE-2012. p. 36.
- 11) Sugimoto, K.; Yajima, H.; Aihara, S.; Yoshinari, H.; Hirota, K.; Toyoda, M.; Kiyosue, T.; Inoue, T.; Handa, T.; Kawabata, T.; Tani, T.; Usami, A. ISOPE-2012. p. 44.
- 12) "Guidelines on Brittle Crack Arrest Design." Nippon Kaiji Kyokai. 2009.
- 13) "Requirements for Use of Extremely Thick Steel Plates." IACS. UR S33, 2013-01.
- 14) Tsuyama, S.; Takeuchi, Y.; Nishimura, K.; Handa, T. Quarterly Journal of the Japan Welding Society. 2012-02, vol. 30, p. 188.
- 15) Handa, T.; Igi, S.; Endo, S.; Tsuyama, S.; Shiomi, H. Quarterly Journal of the Japan Welding Society. 2012-03, vol. 30, p. 213.
- 16) Mimura, H. Journal of High Pressure Institute of Japan. 1993-02, vol. 31, p. 58.